THERMO-ECONOMIC AND ENVIRONMENTAL ASSESSMENT OF A HYBRID SOLAR POWER PLANT WITH A PACKED-BED THERMAL STORAGE AND A SUPERCRITICAL ORC POWER BLOCK

Mabrouk M.T.*, Kheiri A. and Feidt M.
*Author for correspondence
Laboratoire d'Energétique et de Mécanique Théorique et Appliquée,
Université de Lorraine,
Vandoeuvre-lès-Nancy 54500,
France,
E-mail: mohamed-tahar.mabrouk@univ-lorraine.fr

ABSTRACT

In this paper, an optimization-oriented model of a hybrid solar power plant is proposed. The facility is composed of a parabolic trough solar field, a packed bed thermal storage, a fired heater and a supercritical ORC power block.

In a first step, all the components of the power plant are sized. In a second step, its operation is simulated over a typical year using irradiance data as input which allows to assess the Levelized Cost of Electricity (LCOE) and the amount of CO_2 emitted per kWh produced.

A new analytical model developed by the authors is used to simulate the operation of the heat storage and permits to reduce considerably the computation time. Therefore, the model is suitable to be integrated in stochastic optimization algorithms.

Finally, the effects of the solar field size and the storage tank on the LCOE and CO_2 emission are investigated and it has been found that the shape factor of the packed bed storage (the ratio between the hight and the diameter) is a very important parameter that affects the impact of the storage integration on the LCOE and CO_2 emission levels.

INTRODUCTION

The intermittent availability of renewable energy is the most important issue that hampers their development. This is the case for wind and solar power. Thermal Energy Storage (TES) is one of the solutions that allow to offset the mismatch between solar energy availability and electricity demand. However, this solution does not permit, alone, a continuous operation of the power plant with competitive costs. Hence, using a fired heater in addition to the TES is a solution to achieve a complete availability of the power plant with a lower cost of the produced electric kWh and with less CO_2 emissions than power stations fully driven by fossil-fuel.

The hybrid solar power plant considered in this paper is represented in Fig. 1. The solar field is composed of many rows of Parabolic Trough Collectors (PTC) which is the most mature and cost-effective technology used in thermodynamic solar generation [1, 2].

The thermocline storage system considered in this paper is a vertical tank filled with a heat transfer fluid (HTF) and a solid and porous filler material. During the heat charging process, the hot fluid enters from the top of the tank when

NOMENCLATURE

A	[m^2]	Area
Bi	[-]	Biot number
c	[-]	Mass fraction
C	[$]	Cost
crf	[-]	Capital recovery factor
D	[m]	Diameter
E	[J]	Energy
$G_{b,n}$	[W/m^2]	Direct Normal irradiance (DNI)
H	[m]	Height
K_{θ_i}	[-]	Incidence angle modifier
L_a	[m]	Aperture length
p	[m]	Rows spacing
Pe	[-]	Peclet number
St	[-]	Stanton number
T	[K]	Temperature
v	[m/s]	Fluid Velocity
W_a	[m]	Aperture width

Special characters

θ	[-]	Non dimensional temperature
θ_i	[-]	Incidence angle
ε	[-]	Void fraction
τ	[-]	Non dimensional time
ζ	[-]	Non dimensional spatial coordinate

Subscripts

amb	Ambient
cs	Cold sink
eff	Effective value
gen	Generator
h	High
hs	Hot source
in	Inlet
mot	Pump motor
out	Outlet
ref	Reference
s	Storage
th	Thermal

colder fluid exits from the bottom, and conversely, during the heat discharging process, the cold fluid enters from the bottom when warmer fluid exits from the top. The tank has two fluid distributors placed at the top and the bottom to ensures a uniform flow of the fluid over the sectional area.

The Supercritical Organic Rankine Cycle technology (SORC) is considered as a power block alternative. This technology has gained, recently, more attention due to its increased theoretical efficiency. An ORC is called supercritical if the pressure of the working fluid surpass its critical pressure during the cycle and the main advantage of this over the subcritical cycle is a better match between the cooling curve of the heat source and the heating curve of the working fluid leading to less entropy generation.

The algorithm developed here size all the components of the power plant and, then, simulate the dynamic behavior of the solar power plant over a number of days of the year, which is determined by a sensitivity analysis in order to reduce the approximation error. The Levelized Cost of Electricity (LCOE) and the mass of CO_2 emitted per kWh produced are then calculated and the effect of the integration of the solar field and the heat storage on those criteria are discussed.

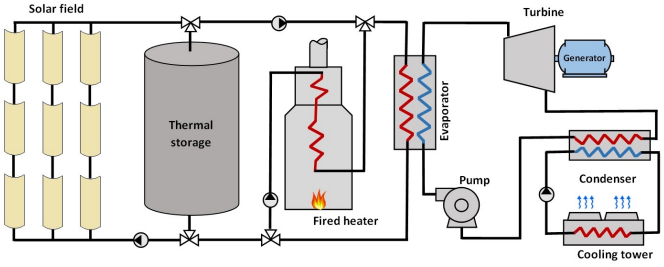

Figure 1: Scheme of the power plant considered in this study

1 Energy management strategy

The hybrid solar power plant is designed to be connected to the grid and to deliver a continuous and constant electric power with a complete reliability. The SORC power block is powered by the HTF wich enters the high pressure HEX at the hot temperature $T_{hs,in}$ and leaves it at the cold temperature $T_{hs,out}$ imposed by the pinch temperature $Pinch_h$ in the HEX.

During sunshine hours, the HTF mass flow rate is regulated in order to keep its temperature at the outlet of the solar field constant and equal to $T_{hs,in}$. This permit a good stratification of the temperature in the heat storage. For a hybrid operation, the energy management strategy which is schematized in Fig. 2 obeys to the following rules :

- If the mass flow rate leaving the solar field is higher than the mass flow rate required for the operation of the ORC, the Rankine cycle takes the energy directly from the solar field and the excess is stored in the storage tank if it is not entirely "filled".
- If, however , the outflow of the solar field is insufficient to supply the power block, it is completed with hot fluid from the storage tank if it is not "empty".
- Otherwise, the hot fluid leaving the solar field is stored and the ORC is fed by the fired heater.

During the charging process the HTF enters from the top of the storage tank at the hot temperature $T_{hs,in}$ and exit from the bottom at the cold temperature $T_{hs,out}$ and the thermocline zone starts to move to the bottom of the tank and when it reaches it, the temperature of the HTF leaving the storage begins to rise. The storage is considered to be entirely filled if the temperature increases by a small fixed amount (eg. 10 °C).

Conversely, during the discharging process, the thermocline zone moves from the bottom to the top and when it reaches the upper exit of the tank the temperature of the discharged fluid begins to decrease. The storage is considered to be entirely empty if the decrease reaches also a small fixed amount.

Knowing this strategy, one can calculate the mass flow rate of the fluid in the storage during each charging or discharging process.

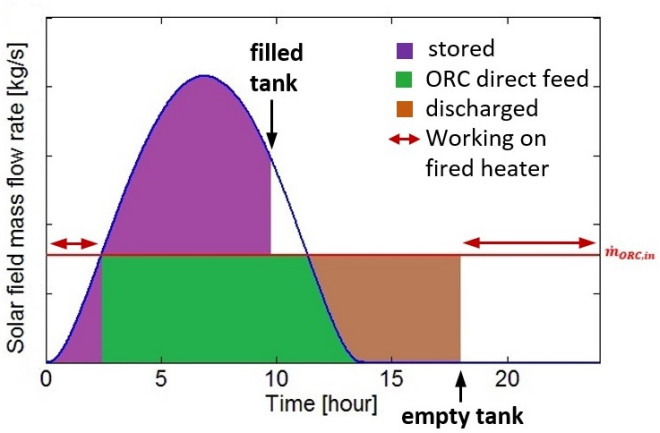

Figure 2: Energy management strategy

2 Solar field model

2.1 Single axis tracking system

A parabolic solar trough system consists of a parabolic reflective surface and an absorber protected by a glass cover. The absorber tube is placed at the focal point of the parabolic surface such that rays reflected by the collector reaches the receiver. A single axis tracking is widely used in solar fields using the Parabolic Trough technology. Therefore, sun rays are not always normal to the aperture plane and their angle with the normal of the aperture plane is known as "incident angle" and denoted by θ_i. The incident angle is a function of the geographic latitude and longitude, the number of the day, the day time and the orientation of the aperture plane and the tracking axis. The

procedure for calculating this angle is widely discussed in the literature [3] and will not be reported here.

2.2 Optical efficiency

The optical efficiency of the collector is defined as the ratio of the energy that reaches the absorber to the energy incident in the collector's aperture. This efficiency is given by:

$$\eta_o(\theta_i)=K_{\theta_i}\ \kappa\ cos(\theta_i) \tag{1}$$

K_{θ_i} is the incidence angle modifier, without the cosine effect, which is approximated by:

$$K_{\theta_i}=1+b_1\theta_i+b_2\theta_i^2 \tag{2}$$

κ is the geometric factor measures the effective reduction of the aperture area of the collector due to shading effect which is a blockage of sun rays caused by the neighboring collectors row that causes a reduction of the reflective area. The fraction of the shaded area was considered to be one-dimensional and is calculated by [4]:

$$f_{bs}=max\left(1-\frac{pcos(\beta)}{W_a},0\right) \tag{3}$$

where W_a and L_a are respectively the width and the length of the collector's aperture, p is the distance between the rows of collectors also called "pitch" and β is the tracking angle. The geometric factor is then defined by:

$$\kappa=1-f_{bs} \tag{4}$$

2.3 Thermal model of the collector

Thermal losses modeling of the receiver is quite discussed in the literature [5, 6]. The thermal resistance model used here is detailed in [7]. It allows to calculate the local thermal efficiency which depends on many variables : the solar irradiance that reaches the receiver per unit of length, the local fluid temperature, the ambient temperature and the velocity of the fluid in the absorber. A correlation of the local efficiency was developed by the authors based on the thermal model [8]. It is written :

$$\eta_{th}=b_1+b_2(T_f-T_{amb})+b_3(T_f-T_{amb})^2 \tag{5}$$

b_1, b_2 and b_3 are constants function of the DNI and the fluid velocity. A multiple polynomial regression is developed for each constant :

$$b_i=\sum_{j,k=0}^{N} c_{jk}v^j\dot{Q}'^k \tag{6}$$

where i=1,2,3 and $\dot{Q}'=\eta_o G_{b,n}W_a$ is the solar irradiance that reaches the receiver per unit of length.

2.4 HTF mass flow rate in the solar field

Since the mass flow rate of the HTF in the solar field is regulated in order to keep a constant temperature at the outlet of the solar field, the mass flow rate $\dot{m}_{row}$ in a row of collectors is calculated using the energy balance equation :

$$\dot{m}_{row}\int_{T_{row,in}}^{T_{row,out}}\frac{c_{p_f}(T)}{\eta_{th}(T)}dT=\eta_o G_{b,n}W_aL_a \tag{7}$$

As seen in eq. (6), the thermal efficiency depends on the flow velocity of the HTF which is unknown. Therefore, an iterative procedure is performed to calculate the mass flow rate. In fact, an initial guess of the flow velocity allows to calculate the mass flow rate and then corrected in the next iteration. Convergence is reached after a few iterations.

3 Thermal storage model

Considering uniform fluid velocity, uniform and isotropic filler material, incompressible fluid, adiabatic walls and constant material properties, the problem can be modeled by a 1D two phases model considering two volume-averaged energy equations respectively for the fluid and the solid filler [9]. These equations can be written in a non dimensional form as follows:

$$\gamma_f\frac{\partial\theta_f}{\partial\tau}+\gamma_f Pe\frac{\partial\theta_f}{\partial\zeta}=\beta_f\frac{\partial^2\theta_f}{\partial\zeta^2}+Bi(\theta_s-\theta_f) \tag{8a}$$

$$\gamma_s\frac{\partial\theta_s}{\partial\tau}=\beta_s\frac{\partial^2\theta_s}{\partial\zeta^2}-Bi(\theta_s-\theta_f) \tag{8b}$$

The scalings applied to the obtain eqs (8a) and (8b) are: $\theta=\frac{T-T_{ref}}{T_{scale}}$, $\tau=\frac{t}{S_t}$ and $\zeta=\frac{z}{L}$ where $S_t=\frac{L^2}{\alpha_{eff}}$ and T_{ref} and T_{scale} are respectively a reference and a scaling constant temperatures selected depending on the application.

The subscript eff refers to the "effective" value of an intrinsic property, e.g. thermal conductivity. Let Φ be an intrinsic property, its effective value is defined as: $\Phi_{eff}=\varepsilon\Phi_f+(1-\varepsilon)\Phi_s$.

The following non-dimensional numbers are used in eqs (8a) and (8b):

$$\gamma_f=\frac{\varepsilon(\rho C_p)_f}{(\rho C_p)_{eff}},\ \gamma_s=\frac{(1-\varepsilon)(\rho C_p)_s}{(\rho C_p)_{eff}},\ \beta_f=\frac{\varepsilon k_f}{k_{eff}}$$

$$\beta_s=\frac{(1-\varepsilon)k_s}{k_{eff}},\qquad Bi=\frac{hL^2}{k_{eff}},\qquad Pe=\frac{vS_t}{L}$$

Eqs (8a) and (8b) are usually solved numerically as in [10–12]. In this case, using a high number of nodes is necessary to avoid numerical diffusion [13].

To tackle this problem, the authors have developed a new model [14]. This model is based on the one phase simplification proposed initially by [15] which uses the perturbation theory. In this approach, the solid temperature is considered as a perturbation of the fluid temperature, $\theta_s = \theta_f + \delta\theta$ with $\delta\theta$ small enough.

Thus, eqs (8a) and (8b) can be replaced by only one equation describing the fluid temperature [15]:

$$\frac{\partial\theta_f}{\partial\tau} + \gamma_f Pe \frac{\partial\theta_f}{\partial\zeta} = (1 + \frac{(\gamma_s\gamma_f Pe)^2}{Bi}) \frac{\partial^2\theta_f}{\partial\zeta^2} \tag{9}$$

Eq (9) is then solved using a Generalized Integral Transforms Technique (GITT) as described in [14]. This new model gives us an analytical solution of the temperature profile at any time and without time stepping when the temperature of the HTF at the entry of the storage is constant and its mass flow rate is time dependent which is the case here. This analytical solution is very useful because a dichotomic search algorithm allows to determine the charge/discharge durations with a few iterations.

4 Organic Rankine Cycle model

4.1 Thermodynamic model of the ORC

The T-s diagram of the supercritical ORC cycle is presented in Fig. 3. The enthalpies of the different points in the diagram can be determined knowing the isentropic eficiencies of the pump and the expander and using the software REFPROP [16,17]:

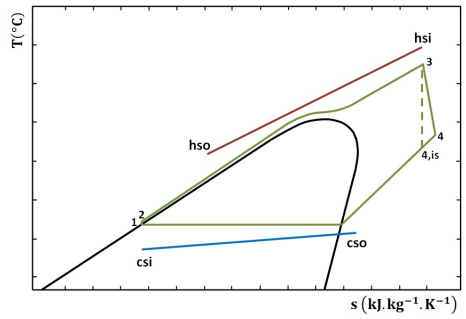

Figure 3: T-s diagram od the supercritical ORC cycle

The required working fluid mass flow rate m_{wf} to produce an electrical power P_{ORC} is calculated by :

$$\dot{m}_{wf} = \frac{P_{ORC}}{\eta_{gen}(h_3 - h_4) - (h_2 - h_1)/\eta_{mot}} \tag{10}$$

4.2 Optimal design of the heat exchangers

The shell-and-tube heat configuration is used for both high and low pressure heat exchangers. Seven geometric parameters must be fixed to size the heat exchangers : the number of the tubes (N_t), number of baffles (N_b), number of tube passes (N_t^p), number of shell passes (N_s^p), the inner diameter of the tubes (D_i), the spacing between tubes (c), and the spacing between baffles (B). The tubes length is calculated in each HEX using the DTLM method. This allows also to calculate the pressure drop in the heat exchanger.

In order to find an optimal sizing of the heat exchanger, its yearly cost is minimized and an optimal set of geometric parameters is found. A nonlinear mixed integer optimization algorithm called NOMAD [18] is used to perform this optimization.

5 Fired heater

5.1 The burner model

Assuming an adiabatic and complete combustion and a negligible mass of water in the fuel the combustion reaction is given by :

$$C_x H_y + (x + \frac{y}{4}) O_2 \longrightarrow x\ CO_2 + \frac{y}{2} H_2O \tag{11}$$

The mass fraction of CO_2 in flue gases is given by [19]:

$$c_{CO_2}^{fg} = \frac{44}{12} . c_C^{fuel} . \frac{m_{fuel}}{1 + m_{fuel}} \tag{12}$$

c_C^{fuel} is the mass fraction of the carbon in the fuel and m_{fuel} is the following ratio :

$$\frac{\dot{m}_{fuel}}{\dot{m}_{fuel} + \dot{m}_{air}} \tag{13}$$

5.2 Energy balance of the fired heater

The energy balance of the fired heater is :

$$\dot{Q}_{comb} + \dot{Q}_{air} + \dot{Q}_{fuel} = \dot{Q}_{setting} + \dot{Q}_{fluid} + \dot{Q}_{fg} \tag{14}$$

$\dot{Q}_{comb}$, $\dot{Q}_{air}$, $\dot{Q}_{fuel}$ and $\dot{Q}_{fg}$ are respectively the combustion energy, the air and fuel enthalpy at the entrance of the burner and the enthalpy of the flue gases at the stack.

Equation (14) allows to calculate the mass flow rate of the fuel consumed by the fired heater in operation :

$$\dot{m}_{fuel} = \dot{m}_f Cp_f (T_{f,out} - T_{f,in}) / \Theta \tag{15}$$

with

$$\begin{aligned} \Theta = & (1-\alpha) LHV_{fuel} + Cp_{fuel}(T_{fuel} - T_{ref}) \\ & + (1+E) S Cp_{air}(T_{air} - T_{ref}) \\ & - (1 + (1+E)S) Cp_{fg}(T_{fg} - T_{ref}) \end{aligned} \tag{16}$$

LHV_{fuel} is the lower heating value of the fuel, α is the fraction of the setting losses, T_{ref} is a reference temperature, E is the air excess factor and S is the fuel-air stoichiometric ratio.

6 Criteria evaluation methodology

The methodology adopted in this paper to evaluate the economic and environmental criteria is presented in Fig. 4. The duration of the fired heater operation t_{fired} is calculated, in accordance with the energy management strategy, after the simulation of the solar block (solar field + heat storage). The annual fuel consumption and CO_2 emission are then calculated using the fired heater model detailed in section 5. The economic criterion is calculated using the following equation :

$$LCOE = \frac{crf.C_{inv} + C_{o\&m} + C_{fuel}}{E_t} \quad (17)$$

Where C_{inv} is the total capital cost, $C_{o\&m}$ is the yearly operation and maintenance cost, C_{fuel} the fuel cost, E_t is the annual electrical energy produced and crf is the capital recovery factor. Capital cost correlations used to evaluate the LCOE can be found in the literature [20]. Each correlation was updated to take into account the currency change and inflation.

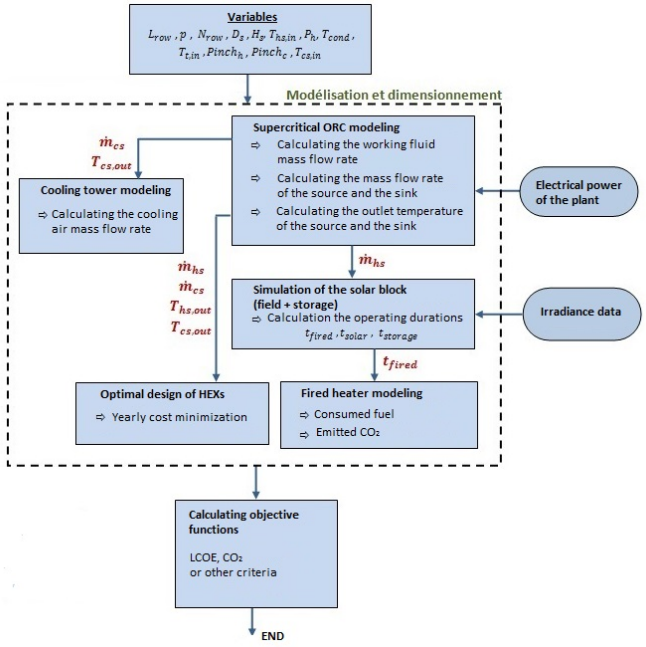

Figure 4: Algorithm for the criteria assessment

7 Results and discussion

7.1 Effect of the number of simulated days on the accuracy of the results

In this section, a 100 MW hybrid power plant is considered as a case study and toluene is chosen as working fluid for the ORC power block. Since the number of simulated days affects directly the computation time, three simulations were performed. In the first case a whole year was simulated. In the second, only 73 days per year regularly spaced were simulated and only 36 days were simulated in the third case. The annual operating duration of the power plant on each mode (on fired heater, on solar field and on fired heater) were calculated for the two latter cases by a linear extrapolation. Results are shown in Fig. 5 and show that the deviation is very small and that there is no need to simulate a whole year to obtain accurate results.

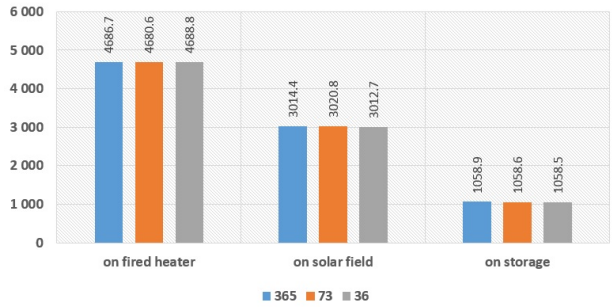

Figure 5: Influence of the number of simulated days on the calculated durations

7.2 Effect of the solar field integration on the economic and environmental criteria

The Algorithm detailed in Fig.4 was used to calculate the LCOE and the yearly CO_2 emission of a 100 MW hybrid power plant. When the number of collector rows is constant, the effect of their length on these the economic and the environmental criteria is shown in Fig. 6. It can be seen, in this case, that the CO_2 emission converge towards an asymptote at around 0.58 kg/kWh. In fact, this asymptote is caused by the fixed size of the storage tank and it is useless to increase the size of the solar field if the storage tank is too small to store all the collected energy.

7.3 Effect of the storage tank integration on the economic and environmental criteria

In Fig. 7, the LCOE and the CO_2 emission are plotted against the storage hight for different base diameters. This figure shows that, for the same size of solar field, The CO_2 emission reduction is highly dependent to the diameter of the tank. For example, it can be seen that for D_s=10m CO_2 emission and LCOE converge towards asymptotes respectively at 0.82 kg/kWh and 0.18 $/kWh. For D_s=35m CO_2 and LCOE can be reduced in best cases to 0.61 kg/kWh and 0.163 $/kWh and for D_s=50m these to criteria cannot be reduced to less than 0.62 kg/kWh and 0.166 $/kWh. Obviously, there is an optimal diameters that allow maximal reductions of CO_2 emission and LCOE. In fact, if the diameter of the tank is small, the flow velocity of the HTF is high and the advection phenomena in the tank is important.

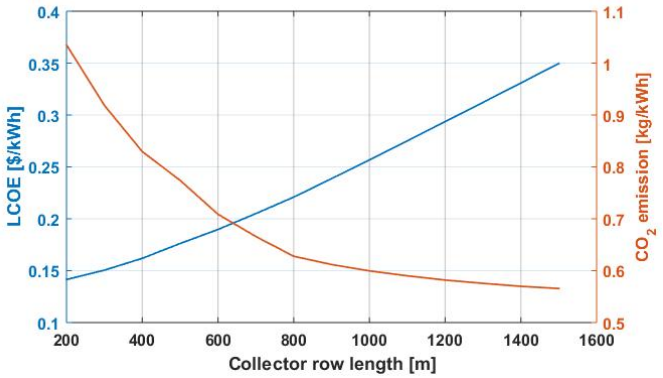

Figure 6: LCOE and CO_2 emission vs Collector row length ; N_{row}=1000, p=10, D_s=15m, H_s=4, $T_{hs,in}$=350°C, P_h=1.2P_{crit}, T_{cond}=60°C, $T_{t,in}$=320°C, $Pinch_h$=$Pinch_c$=10°C, $T_{cs,in}$=30°C

In this case, the thermocline zone displacement is fast. On the contrary, if the diameter of the tank is very big, the axial conduction is bigger causing the enlargement of the thermocline zone. In both cases, the effective capacity of the storage tank is reduced.

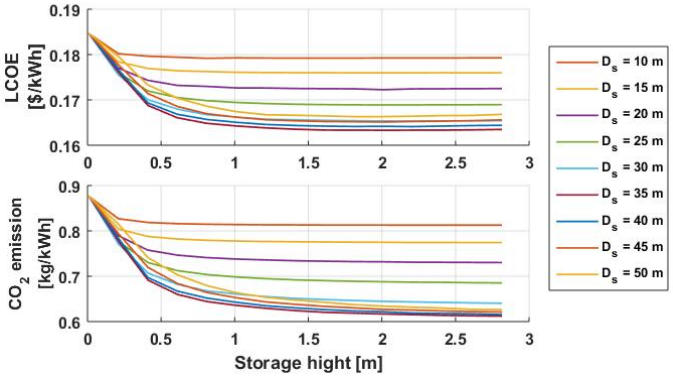

Figure 7: LCOE and CO_2 emission vs storage hight ; L_{row}=500 m,N_{row}=1000, p=10, $T_{hs,in}$=350°C, P_h=1.2P_{crit}, T_{cond}=60°C, $T_{t,in}$=320°C, $Pinch_h$=$Pinch_c$=10°C, $T_{cs,in}$=30°C

To investigate further this aspect, CO_2 emission and LCOE maps are given in figures 8 and 9 as a function of the volume of the storage tank and the shape factor (H_s/D_s). Minimal values of the economic and the environmental criteria are given on these figures and it turns out that the economic minimum allows a good environmental footprint. In fact, at the economic minimum, the design is expected to reject only 9 grams per kWh more than the design at the environmental minimum.

CONCLUSION

In this paper, a hybrid solar power plant with a packed bed thermocline heat storage was considered. An optimization-oriented model was developed in order to perform an economic and environmental assessment of the power plant (LCOE and CO_2 emission). The operation of the solar block (solar field + heat storage) is simulated and the operation duration on each mode is calculated (on solar field, on storage and on fired heater). A model developed by the authors based on the perturbation theory and the Generalized Integral Transforms Technique is used to reduce the simulation computing time and make the model suitable to be introduced in optimization routines. The effect of the solar field size and the storage volume is discussed and it turns out that for each field size an optimal design of the heat storage exists and that the shape factor of the tank is a very important parameter that affects considerably CO_2 and LCOE reduction.

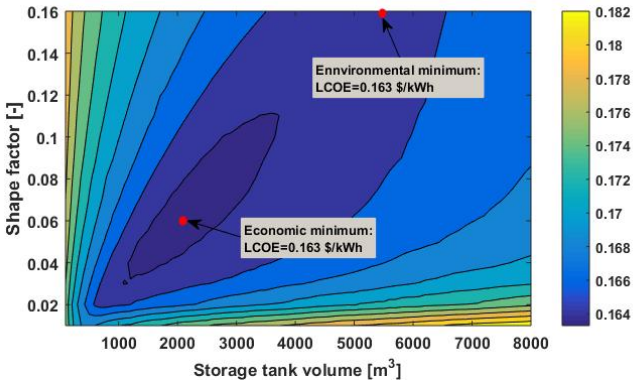

Figure 8: LCOE as a function of the Storage tank volume and the shape factor ; L_{row}=500 m,N_{row}=1000, p=10, $T_{hs,in}$=350°C, P_h=1.2P_{crit}, T_{cond}=60°C, $T_{t,in}$=320°C, $Pinch_h$=$Pinch_c$=10°C, $T_{cs,in}$=30°C

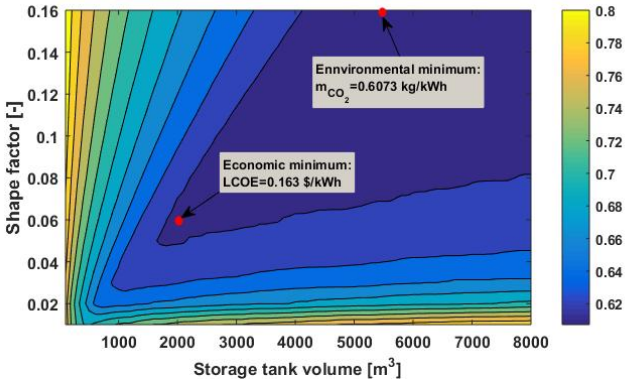

Figure 9: CO_2 emission as a function of the Storage tank volume and the shape factor ; L_{row}=500 m,N_{row}=1000, p=10, $T_{hs,in}$=350°C, P_h=1.2P_{crit}, T_{cond}=60°C, $T_{t,in}$=320°C, $Pinch_h$=$Pinch_c$=10°C, $T_{cs,in}$=30°C

REFERENCES

[1] Price H., Lüpfert E., Kearney D., Zarza E., Cohen G., Gee R., and Mahoney R., Advances in Parabolic Trough Solar Power Technology, *Journal of Solar Energy Engineering*,

vol. 124, no. 2, 2002, pp. 109–125

[2] Arasu A.V. and Sornakumar T., Design, manufacture and testing of fiberglass reinforced parabola trough for parabolic trough solar collectors, *Solar Energy*, vol. 81, no. 10, 2007, pp. 1273 – 1279

[3] Padilla R., *Simplified Methodology for Designing Parabolic Trough Solar Power Plants*, Ph.D. thesis, University of South Florida, 2011

[4] Silva R., Berenguel M., Pérez M., and Fernández-Garcia A., Thermo-economic design optimization of parabolic trough solar plants for industrial process heat applications with memetic algorithms, *Applied Energy*, vol. 113, 2014, pp. 603 – 614

[5] Padilla R.V., Demirkaya G., Goswami D.Y., Stefanakos E., and Rahman M.M., Heat transfer analysis of parabolic trough solar receiver, *Applied Energy*, vol. 88, no. 12, 2011, pp. 5097 – 5110

[6] He Y.L., Xiao J., Cheng Z.D., and Tao Y.B., A MCRT and FVM coupled simulation method for energy conversion process in parabolic trough solar collector, *Renewable Energy*, vol. 36, no. 3, 2011, pp. 976 – 985

[7] Kalogirou S.A., A detailed thermal model of a parabolic trough collector receiver, *Energy*, vol. 48, no. 1, 2012, pp. 298 – 306. 6th Dubrovnik Conference on Sustainable Development of Energy Water and Environmental Systems, SDEWES 2011

[8] Mabrouk M., Optimal energy delivery at a small community scale : application to the optimization of a hybrid solar power plant producing electricity and heat, ph.d. thesis (in french), university of lorraine, 2015

[9] Nakayama A., Kuwahara F., Sugiyama M., and Xu G., A two-energy equation model for conduction and convection in porous media, *International Journal of Heat and Mass Transfer*, vol. 44, no. 22, 2001, pp. 4375 – 4379

[10] Li P., Lew J.V., Karaki W., Chan C., Stephens J., and Wang Q., Generalized charts of energy storage effectiveness for thermocline heat storage tank design and calibration, *Solar Energy*, vol. 85, no. 9, 2011, pp. 2130 – 2143

[11] Li P., Lew J.V., Chan C., Karaki W., Stephens J., and O'Brien J., Similarity and generalized analysis of efficiencies of thermal energy storage systems, *Renewable Energy*, vol. 39, no. 1, 2012, pp. 388 – 402

[12] Bindra H., Bueno P., Morris J.F., and Shinnar R., Thermal analysis and exergy evaluation of packed bed thermal storage systems, *Applied Thermal Engineering*, vol. 52, no. 2, 2013, pp. 255 – 263

[13] Powell K.M. and Edgar T.F., An adaptive-grid model for dynamic simulation of thermocline thermal energy storage systems, *Energy Conversion and Management*, vol. 76, no. 0, 2013, pp. 865 – 873

[14] Mabrouk M., Kheiri A., and Feidt M., Using Generalized Integral Transforms to solve a perturbation model for a packed bed thermal energy storage tank, *International Journal of Heat and Mass Transfer*, vol. 84, 2015, pp. 633–641

[15] Votyakov E.V. and Bonanos A.M., A perturbation model for stratified thermal energy storage tanks, *International Journal of Heat and Mass Transfer*, vol. 75, no. 0, 2014, pp. 218 – 223

[16] Le V., Feidt M., Kheiri A., and Pelloux-Prayer S., Performance optimization of low-temperature power generation by supercritical ORCs (organic rankine cycles) using low GWP (global warming potential) working fluids, *Energy*, vol. 67, 2014, pp. 513 – 526

[17] Le V., Kheiri A., Feidt M., and Pelloux-Prayer S., Thermodynamic and economic optimizations of a waste heat to power plant driven by a subcritical ORC (organic rankine cycle) using pure or zeotropic working fluid, *Energy*, vol. 78, 2014, pp. 622 – 638

[18] Audet C., Le Digabel S., and Tribes C., *NOMAD user guide*, Tech. Rep. G-2009-37, Les cahiers du GERAD, 2009

[19] Spelling J., *Hybrid SolarGas-Turbine Power Plants - A Thermoeconomic Analysis*, Ph.D. thesis, KHT Royal Institute of Thechnology, 2013

[20] Shirazi A., Najafi B., Aminyavari M., Rinaldi F., and Taylor R., Thermal-economic-environmental analysis and multi-objective optimization of an ice thermal energy storage system for gas turbine cycle inlet air cooling, *Energy*, vol. 69, 2014, pp. 212 – 226